

# Driven dipole oscillations and the lowest energy excitations of strongly interacting lattice bosons in a harmonic trap

K. He,<sup>1,2</sup> J. Brown,<sup>2</sup> S. Haas,<sup>3,4</sup> and M. Rigol<sup>1</sup>

<sup>1</sup>*Department of Physics, The Pennsylvania State University, University Park, Pennsylvania 16802, USA*

<sup>2</sup>*Department of Physics, Georgetown University, Washington, DC 20057, USA*

<sup>3</sup>*Department of Physics & Astronomy, University of Southern California, California 90089, USA*

<sup>4</sup>*School of Engineering and Science, Jacobs University Bremen, Bremen 28759, Germany*

We show that the analysis of the time evolution of the occupation of site and momentum modes of harmonically trapped lattice hard-core bosons, under driven dipole oscillations, allows one to determine the energy of the lowest one-particle excitations of the system in equilibrium. The analytic solution of a single particle in the absence of a lattice is used to identify which function of those time-dependent observables is best fit for the analysis, as well as to relate the dynamic response of the system to its single-particle spectrum. In the presence of the lattice and of multiple particles, a much richer and informative dynamical response is observed under the drive.

PACS numbers: 03.75.Kk, 03.75.-b, 67.85.-d, 05.30.Jp

## I. INTRODUCTION

Ultracold atomic gases in one-dimensional (1D) geometries exhibit a rich phenomenology [1] and display remarkable nonequilibrium phenomena [2–4]. They have been the center of much recent experimental and theoretical interest because of the possibility of controlling the potentials used to trap and manipulate these gases and studying their coherent dynamics [5]. For example, using optical lattices, experimentalists have accessed the strongly interacting Tonks-Girardeau regime in 1D bosonic systems [6, 7] and examined their dynamics [2].

In addition to being of interest in their own right [8, 9], the dynamics of strongly correlated one-dimensional systems can be used to probe equilibrium properties not otherwise accessible. For example, the energy absorption rates obtained during the modulation of the amplitude [10–12] and phase [13] of an optical lattice have been used to gain insights into the spectrum of energy excitations in multiple phases of one-dimensional bosonic systems. Unfortunately, long simulation times and the need for independent calculations for each probed frequency have been a major obstacle for unbiased numerical studies of the lowest energy excitations in trapped lattice systems.

Here, we explore an alternative route that allows us to address those challenges. We examine the dynamics of site and momentum occupations of 1D lattice hard-core bosons (HCBs) under driven dipole oscillations. The time-dependent Hamiltonian of interest has the form

$$\begin{aligned}\hat{H}(t) &= \hat{H}_0 + \hat{H}_1(t), \\ \hat{H}_0 &= -J \sum_{i=1}^{L-1} (\hat{b}_i^\dagger \hat{b}_{i+1} + \text{H.c.}) + V \sum_{i=1}^L \left(i - \frac{L+1}{2}\right)^2 \hat{n}_i, \\ \hat{H}_1(t) &= 2VA \sin(\omega't) \sum_{i=1}^L \left(i - \frac{L+1}{2}\right) \hat{n}_i,\end{aligned}\quad (1)$$

where  $\hat{b}_i^\dagger$  ( $\hat{b}_i$ ) is the creation (annihilation) operator of a

HCB at site  $i$  (satisfying the constraints  $\hat{b}_i^2 = \hat{b}_i^{\dagger 2} = 0$ ),  $\hat{n}_i = \hat{b}_i^\dagger \hat{b}_i$  is the site occupation operator,  $J$  is the nearest-neighbor hopping parameter,  $V$  is the strength of the harmonic trapping potential,  $A$  is the amplitude of the driving,  $\omega'$  is its frequency, and  $L$  is the number of lattice sites ( $A \ll L$ ). Note that the part of the Hamiltonian [Eq. (1)] that gives the potential energy is the expansion, up to the linear term, of  $V \sum_{i=1}^L [i - \frac{L+1}{2} + A \sin(\omega't)]^2 \hat{n}_i$ . As such, it can be generated in experiments by either directly adding a linear time-dependent potential or by means of a small periodic displacement of the center of the trap; both generate dipole oscillations. In the absence of a drive, dipole oscillations of bosons in optical lattices have already been studied experimentally [14] and theoretically [15–22].

We show that the parametric excitations due to the aforementioned driving and their signatures in the considered observables provide insight into the lowest-energy excitations of the *global* spectrum of the system. The exposition is organized as follows. In Sec. II, we describe the numerical approach used. In Sec. III, we discuss the single particle solution, followed by the general numerical analysis of the many-particle case in Sec. IV. The conclusions are presented in Sec. V.

## II. NUMERICAL APPROACH

The time evolution of the site and momentum occupations are computed by mapping hard-core bosons onto noninteracting spinless fermions and using properties of Slater determinants as discussed in detail in Refs. [23–25]. This approach is exact, and the computation times involved scale polynomially with system size, which allows us to study large systems for long times. Since the Hamiltonian (1) is time dependent (not the case in Refs. [23–25]), we use a second-order Trotter-Suzuki decomposition [26–28] to compute the time evolution of the

wave function,

$$|\Psi(t + \delta t)\rangle = e^{-\frac{i}{\hbar} \frac{\hat{H}_1(t + \frac{\delta t}{2})}{2} \delta t} e^{-\frac{i}{\hbar} \hat{H}_0 \delta t} e^{-\frac{i}{\hbar} \frac{\hat{H}_1(t + \frac{\delta t}{2})}{2} \delta t} |\Psi(t)\rangle, \quad (2)$$

which introduces an error  $O(\delta t^3)$  [28].  $|\Psi(t + \delta t)\rangle$  can be efficiently calculated in our case because  $e^{-\frac{i}{\hbar} \hat{H}_0 \delta t}$ , being time independent, needs to be computed only once (it is done exactly by diagonalizing  $\hat{H}_0$ ). This leaves the trivial computation of  $e^{-\frac{i}{\hbar} \frac{\hat{H}_1(t + \frac{\delta t}{2})}{2} \delta t}$ , from the already diagonal  $\hat{H}_1(t)$ , to be done at each time step.

In our calculations, we consider  $L = 101$ ,  $V/J = 0.0036$ ,  $A = 1$ , and  $\delta t = 0.005\hbar/J$ . At  $t = 0$ , the system is taken to be in the ground state of  $\hat{H}_0$ , and we simulate the time evolution up to  $t = 5000\hbar/J$ . To assess the accuracy of the results, we computed the overlap between the wavefunctions obtained using the above value of  $\delta t$  and twice that value, at the latest time simulated. For the maximal number of particles considered ( $N_p = 50$ ), the absolute value of that overlap is 0.99999992. This gives us confidence in the high accuracy of our calculations.

### III. ONE-PARTICLE SOLUTION

We start our study of the time evolution of the site occupancies and momentum distributions by analyzing their dynamics for a single particle under the proposed driving. In the presence of a lattice, the low-energy single-particle excitation spectrum of a system in which  $V \ll J$ , such as ours, resembles that of a harmonically trapped system in the continuum [29]. This means that under the assumption of a weak driving away from resonance (so that only the lowest-energy excitations in the lattice are involved), we can gain insights into this system by studying it in the continuum. The Schrödinger equation in this case reads

$$i\hbar \frac{\partial \psi}{\partial t} = -\frac{\hbar^2}{2m} \frac{\partial^2 \psi}{\partial x^2} + \frac{m\omega_0^2 x^2}{2} \psi - m\omega_0^2 A a \sin(\omega' t) x \psi, \quad (3)$$

where  $a$  is the lattice spacing [in Eq. (1), the amplitude of the driving was given in units of the lattice spacing],  $m$  is the mass of the particle, and  $\omega_0$  is the frequency of the trapping potential. The latter two are related to the lattice parameters by the expressions  $m = \hbar^2/2Ja^2$  and  $\omega_0^2 = 4VJ/\hbar^2$ .

Equation (3) admits an exact analytical solution of the form (up to a constant prefactor) [30]

$$\psi(x, t) = \exp \left\{ \frac{i}{2\hbar} [m\omega_0 \alpha(t) x^2 + 2m\omega_0 x_0 \beta(t) x + \hbar \gamma(t)] \right\}, \quad (4)$$

where  $x_0 = \sqrt{\hbar/m\omega_0}$  is the harmonic oscillator characteristic length and the dimensionless parameters

$\alpha(t)$ ,  $\beta(t)$ , and  $\gamma(t)$  satisfy the equations

$$\begin{aligned} \frac{d\alpha(t)}{dt} &= -\omega_0 \alpha(t)^2 - \omega_0, & \frac{d\gamma(t)}{dt} &= \omega_0 \alpha(t) - \omega_0 \beta(t)^2, \\ \frac{d\beta(t)}{dt} &= -\omega_0 \alpha(t) \beta(t) + \omega_0 B \sin(\omega' t), \end{aligned} \quad (5)$$

where  $B = Aa/x_0$  is also a dimensionless parameter. Given our initial condition that  $\psi(x, t = 0)$  is the ground state of the harmonic oscillator, the above set of equations admits a straightforward solution;  $\alpha(t) = i$ . The expressions for  $\beta(t)$  and  $\gamma(t)$  are lengthy and not particularly informative (beyond telling us that the motion is periodic and that the condition for resonance is  $\omega' = \omega_0$ ). However, if we focus on the behavior of  $\varrho(t) = \ln |\psi(x = 0, t)|^2 \propto -\text{Im}[\gamma(t)]$ , we obtain

$$\varrho(t) = \varrho(0) - \frac{B^2 \omega_0^2}{(\omega_0^2 - \omega'^2)^2} [\omega' \sin(\omega_0 t) - \omega_0 \sin(\omega' t)]^2, \quad (6)$$

which is remarkably simple and has a frequency Fourier transform equal to a sum of Dirac  $\delta$  functions at  $\omega = 0, \pm 2\omega_0, \pm 2\omega', \pm(\omega_0 - \omega')$ , and  $\pm(\omega_0 + \omega')$ . Selecting  $\omega' < \omega_0$ , as we do in the following, means that a Fourier transform will produce  $\delta$  functions at the positive frequencies (i)  $\omega = \omega_0 \pm \omega'$ , which allows us to identify the lowest excitation in the spectrum of the harmonic oscillator, (ii)  $\omega = 2\omega_0$ , which allows us to identify the second lowest excitation, and (iii)  $\omega = 2\omega'$ , which is related to the driving frequency.

Furthermore, the momentum Fourier transform of Eq. (4) has a simple form, whose expression at zero momentum (up to a constant prefactor) reads

$$\psi(p = 0, t) = \frac{1}{\sqrt{-i\alpha(t)}} \exp \left[ -\frac{i}{2} \left( \frac{\beta(t)^2}{\alpha(t)} - \gamma(t) \right) \right]. \quad (7)$$

Since in our case  $\alpha(t) = i$ , we can define the quantity  $\varsigma(t) = \ln |\psi(p = 0, t)|^2 \propto -\text{Im}[i\beta(t)^2 + \gamma(t)]$ , which reads

$$\varsigma(t) = \varsigma(0) - \frac{B^2 \omega_0^2 \omega'^2}{(\omega_0^2 - \omega'^2)^2} [\cos(\omega_0 t) - \cos(\omega' t)]^2. \quad (8)$$

The Fourier transform of  $\varsigma(t)$  is a sum of Dirac  $\delta$  functions at the same frequencies as those for  $\varrho(t)$ . It is important to notice that the functions  $\varrho(t)$  and  $\varsigma(t)$  are even functions of  $t$ . This time symmetry is expected because the reflection symmetry of the initial state about  $x = 0$  and  $p = 0$  means that the probability of finding the particle at  $x = 0$  or  $p = 0$  in the driven system must be independent of the sign in the last term in Eq. (3). In order to simplify the exposition, in what follows we set  $\hbar = 1$ .

### IV. MANY-PARTICLES IN A LATTICE

We now study numerically what happens in the presence of a lattice as the number of particles  $N_p$  in the trap is increased. Since this model can be mapped onto non-

interacting spinless fermions [31], its spectrum of excitations coincides with that of the noninteracting fermions. The many-body ground state is created by occupying the lowest  $N_p$  single-particle energy eigenstates, with energies  $E(0)$  through  $E(N_p - 1)$  [ $E(0)$  being the single-particle ground-state energy]. The first (one-particle) excitation corresponds to  $E_1(N_p) = E(N_p) - E(N_p - 1)$ . The second one corresponds to  $E_2(N_p) = E(N_p + 1) - E(N_p - 1)$ , which (particularly at low fillings) is nearly degenerate with  $E'_2(N_p) = E(N_p) - E(N_p - 2)$ . Since a straightforward implementation of our approach does not resolve the difference between  $E_2(N_p)$  and  $E'_2(N_p)$ , we treat them as one and only report  $E_2(N_p)$ . The next-lowest one-particle excitation is  $E_3(N_p) = E(N_p + 2) - E(N_p - 1)$ , which is nearly degenerate with  $E'_3(N_p) = E(N_p + 1) - E(N_p - 2)$  and  $E''_3(N_p) = E(N_p) - E(N_p - 3)$  [again, we only report  $E_3(N_p)$ ], and so on. In the absence of a lattice all excitations would be multiples of  $\omega_0$ , but the lattice changes this dramatically. As discussed in Ref. [29], as  $N_p$  increases,  $E_1(N_p)$  decreases until it vanishes. At that point doubly degenerate eigenstates appear. They have zero weight over a growing region in the center of the trap and are related to the emergence of an  $n_i = \langle \hat{n}_i \rangle = 1$  insulator [29]. As a result, multiple properties of the lattice system are qualitatively different from those in the continuum [18, 29, 32–34].

In Fig. 1(a), we show  $E_1$ ,  $E_2$ , and  $E_3$  vs  $N_p$  for our system at  $t = 0$ . As expected, for small values of  $N_p$ , they are approximately equal to  $\varepsilon_0 l$ , where  $\varepsilon_0 = \omega_0$  and  $l = 1, 2$ , and  $3$ , and decrease with increasing  $N_p$ . Degeneracies set in for  $N_p \geq 46$ . At those fillings, a Mott insulator with  $n_i = 1$  can be seen in the ground-state site occupancies, as shown in the inset in Fig. 1(a). Figure 1(b) depicts the frequencies at which the Fourier transform of the time evolution of the central site occupation and that of the zero momentum node should exhibit the largest response with increasing  $N_p$ , according to the single-particle results extended to account for the lattice effects depicted in Fig. 1(a). We take  $\omega' = 0.05J$  to be the driving frequency and  $\omega_0 = 0.12J$  to be the trapping frequency.

In experiments with ultracold gases the momentum distribution function  $m_k$  can be determined in time-of-flight measurements, in which all confining potentials are turned off and the system is allowed to evolve freely [1, 5], while the recent use of very high resolution optical imaging systems has made measuring site occupancies  $n_i$  feasible [35–38]. In what follows, we focus on the dynamics of those quantities under the drive.

In the insets in Fig. 2, we show the time evolution of the occupation of the site at the trap center  $n_{i=51}$  [inset in Fig. 2(a)] and that of the zero momentum occupation [inset in Fig. 2(b)]. They exhibit periodic dynamics in which multiple frequencies are involved, and at the shortest times  $t > 0$ , both observables decrease as predicted by Eqs. (6) and (8). In our numerical calculations the observables are measured in intervals  $\Delta t = 2J^{-1}$ . In addition, when computing the Fourier transforms of

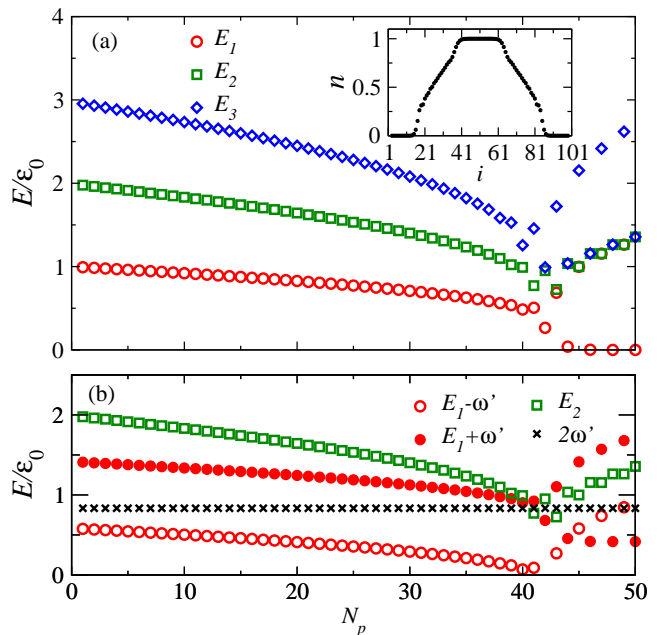


FIG. 1. (Color online) (a) Three lowest one-particle energy excitations as a function of the number of particles in the ground state. The inset shows the site occupancies for  $N_p = 50$ . (b) Expected frequencies for the largest response in the Fourier transform of  $\ln[n_{i=51}(t)]$  and  $\ln[m_{k=0}(t)]$ , which follows from the prediction for one particle in the continuum while taking into account that the spectrum changes because of the presence of a lattice.

$\ln[n_{i=51}(t)]$  and of  $\ln[m_{k=0}(t)]$ , we only considered times in the interval  $500J^{-1} < t \leq 5000J^{-1}$ . By not taking into account results for earlier times, we reduce the effect of any transient behavior that may affect our results.

In the main panels in Fig. 2, we show the Fourier transforms of  $\ln[n_{i=51}(t)]$  [ $N(\omega)$  in Fig. 2(a)] and of  $\ln[m_{k=0}(t)]$  [ $M(\omega)$  in Fig. 2(b)] for a system with  $N_p = 5$ . For both observables, we find that the four most prominent peaks [better seen in  $M(\omega)$  in Fig. 2(b)] are at the frequencies  $\omega_{1,4} = E_1 \mp \omega'$ ,  $\omega_2 = 2\omega'$ , and  $\omega_5 = E_2$  as predicted by the analysis for one particle in the continuum. Note that the values of  $E_1$  and  $E_2$  are those depicted in Fig. 1 for  $N_p = 5$  and were obtained from exactly diagonalizing the Hamiltonian at  $t = 0$ . They depart from the values  $E_1 = \omega_0$  and  $E_2 = 2\omega_0$  expected in the continuum.

In addition to those four frequencies, we find that others are also highlighted by the Fourier analysis as the number of particles is increased. The most prominent ones with signatures in both observables are  $\omega_{3,8} = E_2 \mp 2\omega'$ ,  $\omega_6 = E_1 + 3\omega'$ , and  $\omega_{7,9} = E_3 \mp \omega'$ . We note that  $\omega_{7,9}$  are just signatures of  $E_3$  displaced by  $\mp \omega'$ , respectively, similar to  $\omega_{1,4}$  for  $E_1$ . This means that  $E_3$  can also be identified by analyzing the dynamics in the lattice. Our results also show that other replicas of  $E_1$  can be found to be displaced by  $(2l + 1)$  multiples of  $\omega'$  (where  $l > 0$  is an integer) and those of  $E_2$  can be found to be displaced by  $2l$  multiples of  $\omega'$ . Hence, there is a pattern by which the frequencies of one-particle tran-

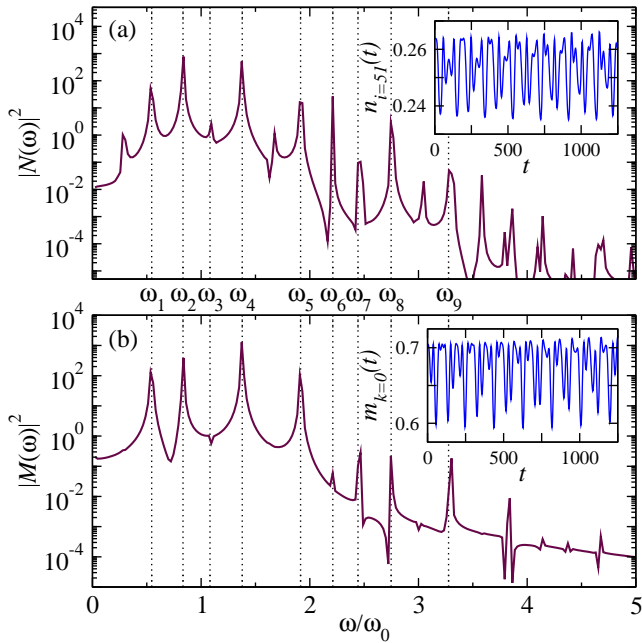


FIG. 2. (Color online) Fourier transform of the time evolution of the occupation of (a) the site at the center of the trap ( $i = 51$ ) and (b) the zero-momentum mode in a system with  $N_p = 5$  HCBs. The inset in each panel depicts the time evolution of the respective observable ( $t$  is given in units of  $J^{-1}$ ). Vertical dashed lines in the main panels indicate the most prominent frequencies highlighted in the Fourier transform of both observables. They correspond to  $\omega_1 = E_1 - \omega'$ ,  $\omega_2 = 2\omega'$ ,  $\omega_3 = E_2 - 2\omega'$ ,  $\omega_4 = E_1 + \omega'$ ,  $\omega_5 = E_2$ ,  $\omega_6 = E_1 + 3\omega'$ ,  $\omega_7 = E_3 - \omega'$ ,  $\omega_8 = E_2 + 2\omega'$ , and  $\omega_9 = E_3 + \omega$ .

sitions that change the parity of the ground state are displaced by odd multiples of  $\omega'$ , while the frequencies of the transitions that do not change the parity of the ground state are displaced by even multiples of  $\omega'$  (including zero). Since we are computing the Fourier transforms of  $\ln[n_{i=51}(t)]$  and of  $\ln[m_{k=0}(t)]$ , this pattern can be understood to be a consequence of the invariance of  $n_{i=51}(t)$  and  $m_{k=0}(t)$  under  $t \rightarrow -t$ , as discussed for the one-particle case. Only specific combinations of periodic functions of  $\omega t$  and  $\omega' t$  appear to ensure that the resulting functions are even in time.

In order to illustrate the effect of larger numbers of particles, we show in Fig. 3 density plots of  $|N(\omega)|^2$  [Fig. 3(a)] and of  $|M(\omega)|^2$  [Fig. 3(b)] vs  $\omega/\omega_0$  and  $N_p$ . Open symbols depict the values of  $\omega_1$  through  $\omega_9$ , introduced in Fig. 2, as a function of the number of particles. Note that for most fillings before the Mott insulator appears in the center of the trap,  $\omega_{1,4}$ ,  $\omega_2$ , and  $\omega_5$  are the frequencies at which both Fourier transforms have their maximal values. Lattice effects are strongest in  $|N(\omega)|^2$ , where, even for the smallest number of particles, frequencies other than  $\omega_{1,2,4,5}$  are highlighted. Furthermore, one can also see lines of high intensity whose frequencies increase with increasing  $N_p$ . For the cases we could identify (not shown), they involve combinations of  $\omega'$  with  $-E_1$  and  $-E_2$ . None of those appear in the analytic solution

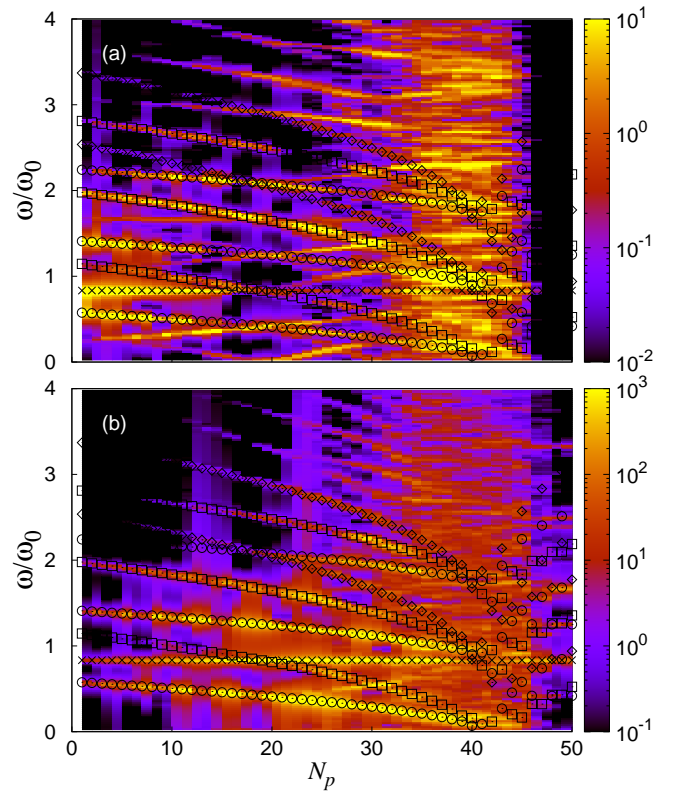


FIG. 3. (Color online) Density plots of (a)  $|N(\omega)|^2$  and (b)  $|M(\omega)|^2$  as a function of  $\omega/\omega_0$  and  $N_p$ . We also report, as open symbols, results for  $\omega_1$  through  $\omega_9$  (see caption in Fig. 2) ordered from bottom to top on the left side of each panel. Note that, following the convention in Fig. 1, results involving  $E_1$  ( $\omega_{1,4,6}$ ) are depicted by circles,  $E_2$  ( $\omega_{3,5,8}$ ) by squares,  $E_3$  ( $\omega_{7,9}$ ) by diamonds, and  $2\omega'$  ( $\omega_2$ ) by crosses.

in the continuum. The results in Fig. 3(a) apply to both HCBs and noninteracting fermions to which HCBs can be mapped, as their site occupancies are identical.

Overall, the best results for the Fourier analysis are obtained for  $|M(\omega)|^2$ , as shown in Fig. 3(b). In that case, most frequencies  $\omega_1$  through  $\omega_9$  are easily identifiable, and lattice effects are the weakest for the lowest fillings, where only  $\omega_{1,2,4,5}$  are clearly seen in Fig. 3(b) [compare with Fig. 1(b)]. When a Mott insulator is present in the center of the trap (fillings above  $N_p = 45$ ), one can see that  $|N(\omega)|^2$  exhibits almost no response (as expected).  $|M(\omega)|^2$ , on the other hand, exhibits a response that is consistent with some of the predictions indicated by the open symbols. This supports the view that a Fourier analysis of  $\ln[m_{k=0}(t)]$ , a quantity that behaves very differently for HCBs and fermions [33, 34], is better suited to study the lowest excitations of the trapped system.

Since HCBs correspond to the  $U/J \rightarrow \infty$  limit of the Bose-Hubbard model (where  $U$  is the on-site interaction), the Fourier analysis of  $\ln[m_{k=0}(t)]$  can become a powerful tool to study single-particle excitations of Bose-Hubbard-like systems in the presence of a harmonic confinement for strong interactions ( $U \gg V, J$ ). As a matter of fact, an exact diagonalization analysis of the Bose-Hubbard

model in the presence of a harmonic trap presented in Ref. [18] showed that, for  $U/J > 10$ , the difference between the lowest-energy excitations of soft-core bosons and hard-core bosons scales as  $J^2/U$ , and the latter accurately describes the dynamics of the former. As such, we expect that the approach discussed here will be relevant to systems with  $U/J > 10$  and fillings  $n \leq 1$  in the center of the trap.

## V. CONCLUSIONS

We have shown that the study of the dynamics of site occupancies and momentum distribution functions of trapped particles under driven dipole oscillations reveals the lowest-energy excitations of the system. The analysis of the momentum distribution function was found to provide the best results for lattice hard-core bosons, and we

expect this to extend to the soft-core case in the presence of strong interactions. As opposed to approaches that use lattice modulations, with this approach one does not need to probe the system under different driving frequencies. We have also studied (not shown) driven systems in which the strength of the confining potential is the one that is periodically modulated. In that case, the lowest excitations that preserve parity can be determined by studying the Fourier transform of the same observables as considered here.

## VI. ACKNOWLEDGMENTS

This work was supported by the Office of Naval Research (K.H. and M.R.) and by Department of Energy Grant No. DE-FG02-05ER46240 (S.H.). We thank Aditya Raghavan and David Weiss for useful discussions.

- 
- [1] M. A. Cazalilla, R. Citro, T. Giamarchi, E. Orignac, and M. Rigol, *Rev. Mod. Phys.* **83**, 1405 (2011).
- [2] T. Kinoshita, T. Wenger, and D. S. Weiss, *Nature* **440**, 900 (2006).
- [3] S. Trotzky, Y.-A. Chen, A. Flesch, I. P. McCulloch, U. Schollwöck, J. Eisert, and I. Bloch, *Nat. Phys.* **8**, 325 (2012).
- [4] M. Gring, M. Kuhnert, T. Langen, T. Kitagawa, B. Rauer, M. Schreitl, I. Mazets, D. A. Smith, E. Demler, and J. Schmiedmayer, *Science* **337**, 1318 (2012).
- [5] I. Bloch, J. Dalibard, and W. Zwerger, *Rev. Mod. Phys.* **80**, 885 (2008).
- [6] T. Kinoshita, T. Wenger, and D. S. Weiss, *Science* **305**, 1125 (2004).
- [7] B. Paredes, A. Widera, V. Murg, O. Mandel, S. Fölling, I. Cirac, G. V. Shlyapnikov, T. W. Hänsch, and I. Bloch, *Nature* **429**, 277 (2004).
- [8] M. Rigol, V. Dunjko, V. Yurovsky, and M. Olshanii, *Phys. Rev. Lett.* **98**, 050405 (2007).
- [9] A. Polkovnikov, K. Sengupta, A. Silva, and M. Vengalattore, *Rev. Mod. Phys.* **83**, 863 (2011).
- [10] A. Iucci, M. A. Cazalilla, A. F. Ho, and T. Giamarchi, *Phys. Rev. A* **73**, 041608 (2006).
- [11] C. Kollath, A. Iucci, T. Giamarchi, W. Hofstetter, and U. Schollwöck, *Phys. Rev. Lett.* **97**, 050402 (2006).
- [12] G. Orso, A. Iucci, M. A. Cazalilla, and T. Giamarchi, *Phys. Rev. A* **80**, 033625 (2009).
- [13] A. Tokuno and T. Giamarchi, *Phys. Rev. Lett.* **106**, 205301 (2011).
- [14] C. D. Fertig, K. M. O'Hara, J. H. Huckans, S. L. Rolston, W. D. Phillips, and J. V. Porto, *Phys. Rev. Lett.* **94**, 120403 (2005).
- [15] A. Polkovnikov and D.-W. Wang, *Phys. Rev. Lett.* **93**, 070401 (2004).
- [16] M. Rigol, V. Rousseau, R. T. Scalettar, and R. R. P. Singh, *Phys. Rev. Lett.* **95**, 110402 (2005).
- [17] J. Ruostekoski and L. Isella, *Phys. Rev. Lett.* **95**, 110403 (2005).
- [18] A. M. Rey, G. Pupillo, C. W. Clark, and C. J. Williams, *Phys. Rev. A* **72**, 033616 (2005).
- [19] G. Pupillo, A. M. Rey, C. J. Williams, and C. W. Clark, *New J. Phys.* **8**, 161 (2006).
- [20] I. Danshita and C. W. Clark, *Phys. Rev. Lett.* **102**, 030407 (2009).
- [21] S. Montangero, R. Fazio, P. Zoller, and G. Pupillo, *Phys. Rev. A* **79**, 041602 (2009).
- [22] I. Danshita, *Phys. Rev. Lett.* **111**, 025303 (2013).
- [23] M. Rigol and A. Muramatsu, *Phys. Rev. Lett.* **93**, 230404 (2004).
- [24] M. Rigol and A. Muramatsu, *Phys. Rev. Lett.* **94**, 240403 (2005).
- [25] M. Rigol and A. Muramatsu, *Mod. Phys. Lett.* **19**, 861 (2005).
- [26] H. F. Trotter, *Proc. Am. Math. Soc.* **10**, 545 (1959).
- [27] M. Suzuki, *Commun. Math. Phys.* **51**, 183 (1976).
- [28] H. De Raedt and B. De Raedt, *Phys. Rev. A* **28**, 3575 (1983).
- [29] M. Rigol and A. Muramatsu, *Phys. Rev. A* **70**, 043627 (2004).
- [30] K. Husimi, *Prog. Theor. Phys.* **9**, 381 (1953).
- [31] E. Lieb, T. Shultz, and D. Mattis, *Ann. Phys. (NY)* **16**, 406 (1961).
- [32] C. Hooley and J. Quintanilla, *Phys. Rev. Lett.* **93**, 080404 (2004).
- [33] M. Rigol and A. Muramatsu, *Phys. Rev. A* **70**, 031603(R) (2004).
- [34] M. Rigol and A. Muramatsu, *Phys. Rev. A* **72**, 013604 (2005).
- [35] W. S. Bakr, J. I. Gillen, A. Peng, S. Fölling, and M. Greiner, *Nature* **462**, 74 (2009).
- [36] W. S. Bakr, A. Peng, M. E. Tai, R. Ma, J. Simon, J. I. Gillen, S. Fölling, L. Pollet, and M. Greiner, *Science* **329**, 547 (2010).
- [37] J. F. Sherson, C. Weitenberg, M. Endres, M. Cheneau, I. Bloch, and S. Kuhr, *Nature* **467**, 68 (2010).
- [38] C. Weitenberg, M. Endres, J. F. Sherson, M. Cheneau, P. Schauß, T. Fukuhara, I. Bloch, and S. Kuhr, *Nature* **471**, 319 (2011).